International Journal of Mass Spectrometry and Ion Processes, 57 (1984) 211–224
Elsevier Science Publishers B.V., Amsterdam – Printed in The Netherlands

SELECTED-ION FLOW TUBE METHODS APPLIED TO THE BRACKETING OF PROTON AFFINITIES. $PA(C_2N_2)$ AND $PA(HC_3N)$

A.B. RAKSIT and D.K. BOHME

Department of Chemistry and Centre for Research in Experimental Space Science, York University, Downsview, Ont. M3J 1P3 (Canada)

(Received 28 November 1983)

ABSTRACT

A selected-ion flow tube (SIFT) apparatus fitted with an electron impact ion source has been used to produce protonated species XH^+ by direct electron impact, by reaction of X^+ with H_2, and by reaction of H_2^+ with X. The three methods of XH^+ production were applied in the bracketing of the proton affinities of cyanogen, C_2N_2, and cyanoacetylene, HC_3N, with measurements of rate constants for proton-transfer reactions of XH^+ with C_2N_2 and HC_3N and of $C_2N_2H^+$ and $H_2C_3N^+$ with X. Comparisons with established proton affinities for X provide values for $PA(C_2N_2) = 162 \pm 2$ kcal mol^{-1} and $PA(HC_3N) = 184 \pm 4$ kcal mol^{-1}. The latter result is in disagreement with a previous flowing afterglow determination.

INTRODUCTION

In a selected-ion flow tube (SIFT) apparatus the ion production and ion reaction regions are separated by a quadrupole mass spectrometer [1]. With a suitable ion source such a configuration allows the separate study of either the forward or the reverse direction of ion/molecule reactions, such as the proton-transfer reaction.

$$XH^+ + Y \rightleftarrows YH^+ + X \qquad (1)$$

Measurements of the forward and reverse rate constants for reaction (1) can provide a determination of the overall standard free energy change and a measure of the difference in the proton affinities of X and Y, $\Delta PA(X, Y)$. We have used this approach previously in the determination of ΔPA for atoms and small molecules, viz. ΔPA (H_2, O_2), ΔPA (Kr, O_2) and ΔPA (H_2, Kr), the protonated species having been generated in a small flowing afterglow tube by ion/molecule reaction at moderate pressures prior to ion selection [2]. SIFT instruments are also commonly fitted with an electron impact ion source operating at lower pressures so that ion/molecule reac-

0168-1176/84/$03.00

tions are suppressed prior to ion selection. For proton affinity studies this can be a disadvantage since desired ions of the type XH^+ are not necessarily produced as daughter ions in the ion source. In the study reported here two other methods of production of XH^+ are explored in which ionization proceeds initially by electron impact at low pressures. The X^+ or H_2^+ ions are selected and manipulated to produce XH^+ by ion/molecule reactions before the ions enter the reaction region. The methods are applied in the bracketing of the proton affinities of cyanoacetylene and cyanogen. These two molecules were chosen because of their role in current models of interstellar cloud and planetary atmospheric ion chemistry [3,4]. Also, the proton affinity of cyanoacetylene has been investigated in traditional flowing afterglow experiments [5] so that we may compare the two methodologies. The flowing afterglow measurements bracketed $PA(HC_3N)$ between $PA(NH_3)$ and $PA(CH_2)$. This result is in conflict with the SIFT measurements reported here. As far as we are aware, there has been no previous report of a value for the proton affinity of cyanogen.

EXPERIMENTAL

The measurements were performed with the selected-ion flow tube/flowing afterglow apparatus at York University [6,7]. For the measurements reported here, the instrument was fitted with an axial electron impact ionizer (Extranuclear, Model 041-3). Several of the XH^+ ions were generated directly in this source by electron bombardment of a suitable parent gas at 25–60 eV: H_2O^+ from water vapour, CH_3^+ from CH_4, $C_2H_3^+$ and C_3H^+ from propylene. Ions generated in this fashion were selected and injected at 8–20 V into helium buffer gas. For $C_2H_3^+$, CH_3^+ and C_3H^+ the spectra observed downstream with the second quadrupole mass spectrometer are included in Fig. 1(a). Ions other than the selected ion may appear downstream as a result of ion/molecule reactions with impurities in the buffer gas or with gas which leaks into the flow tube from the ion source through the selection quadrupole [7]. For $C_2H_3^+$, for example, reactions with H_2O impurity result in the formation of H_3O^+, and reactions with propylene leaking from the source produce $C_3H_7^+$. Background ions were also observed in the case of C_3H^+ but at levels below 0.5% of the C_3H^+ signal [7].

Two other methods of producing XH^+ ions were explored in which X^+ or H_2^+ was the selected ion. When X^+ is injected into H_2 buffer gas formation of XH^+ usually follows directly as a result of hydrogen atom transfer as in

$$X^+ + H_2 \rightarrow XH^+ + H \qquad (2)$$

Spectra generated in this fashion are shown in Fig. 1(b) for $X^+ = H_2^+$, H_2O^+, $C_2H_4^+$, HC_3N^+, $C_2N_2^+$, CH_3OH^+, $CH_3NO_2^+$, $(CH_3)_2CO^+$ and

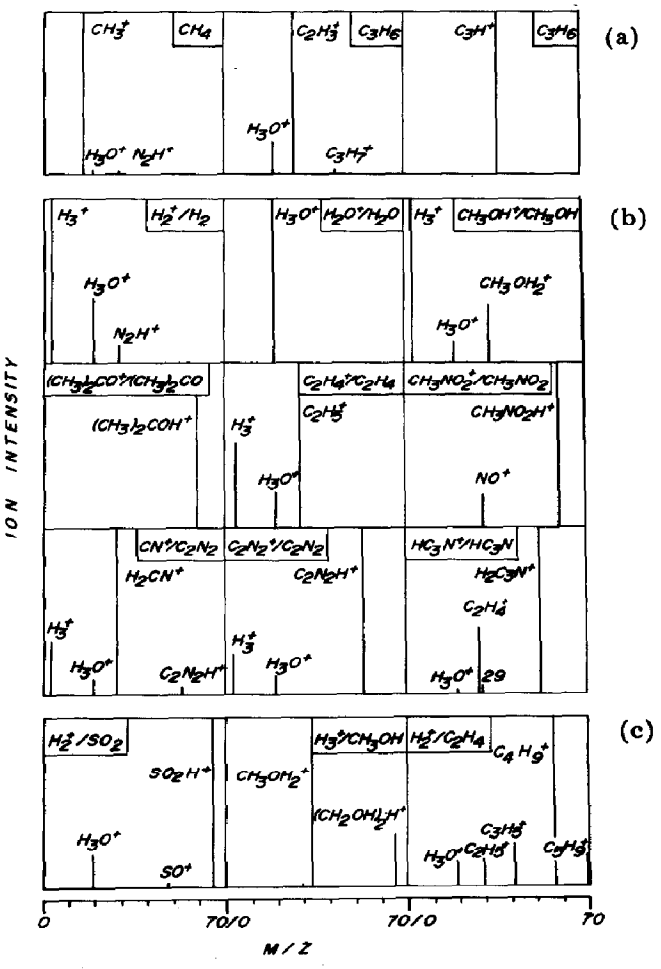

Fig. 1. SIFT spectra recorded downstream for three modes of production of protonated molecules, XH^+. (a) XH^+ derived by electron impact of the parent gas indicated, selected, and injected into helium carrier gas, $P = 0.33$ Torr. (b) X^+ derived by electron impact of the parent gas indicated, selected, and injected into hydrogen carrier gas, $P = 0.19$ Torr. XH^+ produced by ion/molecule reactions with H_2. (c) H_2^+ derived by electron impact of H_2, selected, and injected into hydrogen carrier gas, $P = 0.19$ Torr. The reagent gas indicated is added into the flow tube to produce XH^+ by ion/molecule reactions.

CN^+ in which two successive hydrogen atom transfer reactions establish H_2CN^+. Background ions generated by secondary reactions with impurities in the buffer gas are again evident, e.g. H_3O^+, N_2H^+. Also, in some instances background ions are present which are presumed to result from dissociation: NO^+ from $CH_3NO_2H^+$ [8] and m/z 28 ($C_2H_4^+$) from HC_3N^+ which is dissociated initially to C_2H^+ and CN. Finally, H_3^+ appears as a strong background ion in the spectra for $C_2N_2H^+$, H_2CN^+, $C_2H_5^+$, and especially $CH_3OH_2^+$. It may arise from H_2^+ produced by charge transfer

between X^+ and H_2, particularly when X has a high ionization potential as is the case with CN and C_2N_2. Alternatively, H_3^+ may be produced by direct reaction between H_2 and X^+. Further modification of the ion spectra may result from secondary reactions with source gas which has leaked through the ion selection region.

The second method of generating XH^+ is initiated by injection of H_2^+ into the H_2 buffer gas. The H_2^+ ion reacts with H_2 to form H_3^+ and both ions will react with X which is added upstream in the flow tube. In this way XH^+ can be established by proton transfer from H_3^+ or H_2^+. When X has a moderately high proton affinity, proton transfer will also proceed with impurity ions such as H_3O^+ and N_2H^+ and a very 'clean' spectrum of XH^+ can result although secondary reactions of XH^+ with X may also establish cluster ions of the type $XH^+ \cdot X$. This is evident, for example, in the spectrum for $X = CH_3OH$ shown in Fig. 1(c). Secondary and even tertiary reactions may also give rise to more complex spectra as with $X = C_2H_4$, in which case $C_3H_5^+$, $C_4H_9^+$ and $C_5H_9^+$ are established by reactions (3)–(5).

$$C_2H_5^+ + C_2H_4 \rightarrow C_3H_5^+ + CH_4 \quad (3)$$

$$C_2H_5^+ + C_2H_4 + H_2 \rightarrow C_4H_9^+ + H_2 \quad (4)$$

$$C_3H_5^+ + C_2H_4 + H_2 \rightarrow C_5H_9^+ + H_2 \quad (5)$$

The operating conditions in this latter case begin to approach those which are achieved with the more conventional flowing afterglow method when C_2H_4 is added to a hydrogen afterglow.

The reagent and parent gases and vapours used in this study as well as the helium and hydrogen buffer gases were generally of a high purity, viz. ≥ 99.5 mole%. HC_3N was prepared in the laboratory with methyl propiolate as the starting material [9]. Our experiments with H_3^+ as the 'chemical ionization' reagent indicated purities for HC_3N and C_2N_2 (nominally 98.5% by volume) of greater than 99%. To remove traces of water vapour the helium and hydrogen buffer gases were passed through zeolite traps (a 50 : 50 mixture of Union Carbide molecular sieves 4A and 13X) cooled to liquid nitrogen temperature. All measurements were made at an ambient temperature of 296 ± 2 K.

RESULTS AND DISCUSSION

Reactions with cyanogen

Both proton-transfer and addition reactions were observed to proceed between XH^+ and C_2N_2. Fast proton-transfer reactions were observed with H_3^+, N_2H^+, H_2O^+, $C_2H_3^+$ and SO_2H^+ for which the rate constants are

summarized in Table 1. Data obtained for the fast proton-transfer reaction with H_3^+ are shown in Fig. 2. The N_2H^+ and H_3O^+ ions are present as impurity ions in this case. These data indicate a fast proton-transfer reaction with N_2H^+ and no apparent reaction with H_3O^+. Separate experiments showed that both H_3O^+ and the $C_2N_2H^+$ product add C_2N_2 with an effective second-order rate constant of about 4×10^{-11} cm^3 molecule^{-1} s^{-1} at a total hydrogen pressure of 0.19 Torr and density of 6.1×10^{15} molecules cm^{-3}. $C_2H_3^+$ adduct formation proceeds in competition with proton transfer as shown in Fig. 3. This figure also shows the addition reaction of H_3O^+ with C_2N_2 and the failure of protonated propylene to react with C_2N_2. Separate experiments in which H_3O^+ was established in H_2 buffer gas by adding water vapour provided evidence for the occurrence of the molecular switching reaction

$$H_3O^+ \cdot C_2N_2 + H_2O \rightarrow H_3O^+ \cdot H_2O + C_2N_2 \quad (6)$$

Cyanogen adducts were also observed to be formed in H_2 buffer with $CH_3OH_2^+$, C_3H^+, H_2CN^+ and $C_2H_5^+$. The results obtained with $C_2H_5^+$ are shown in Fig. 4. In this case, H_2^+ was the injected ion and C_2H_4 was added

TABLE 1

Rate constants determined for proton-transfer reactions with $C_2N_2H^+$ or C_2N_2 using the SIFT technique at 296 ± 2 K

Reaction [a]			Buffer gas	k_{obs} [b]/10^{-9} (cm^3 molecule^{-1} s^{-1})
$H_3^+ + C_2N_2$	→	$C_2N_2H^+ + H_2$	H_2	2.2
$N_2H^+ + C_2N_2$	→	$C_2N_2H^+ + N_2$	H_2	1.2
$H_2O^+ + C_2N_2$	→	$C_2N_2H^+ + OH$	He	1.0
$C_2H_3^+ + C_2N_2$	$\xrightarrow{0.8}$	$C_2N_2H^+ + C_2H_2$	He	0.71 [c]
	$\xrightarrow{0.2}$	$C_2H_3^+ \cdot C_2N_2$		
$SO_2H^+ + C_2N_2$	→	$C_2N_2H^+ + SO_2$	H_2	0.82
$C_2N_2H^+ + C_2H_4$	$\xrightarrow{0.7}$	$C_2H_5^+ + C_2N_2$	H_2	0.56 [d]
	$\xrightarrow{0.3}$	$C_2N_2H^+ \cdot C_2H_4$	H_2	
$C_2N_2H^+ + H_2O$	→	$H_3O^+ + C_2N_2$	H_2	0.51
$C_2N_2H^+ + CH_3OH$	→	$CH_3OH_2^+ + C_2N_2$	H_2	1.5

[a] The reactions are listed in order of increasing proton removal energy for the reacting ion or proton affinity of the reacting neutral.

[b] The accuracy of the rate constant is estimated to be better than ± 30%.

[c] $P = 0.33$ Torr, He concentration $= 1.1 \times 10^{16}$ molecules cm^{-3}.

[d] $P = 0.20$ Torr, H_2 concentration $= 6.7 \times 10^{15}$ molecules cm^{-3}.

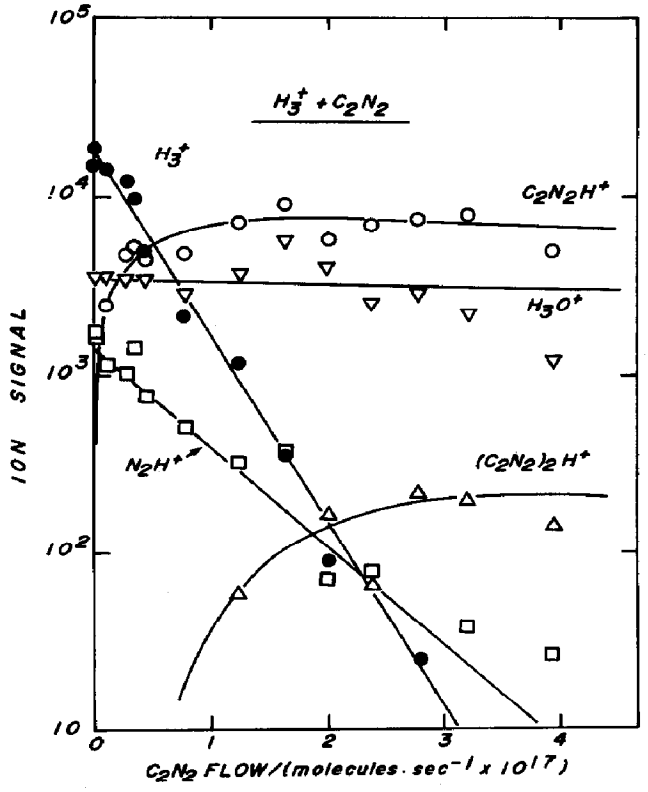

Fig. 2. The observed variation of ion signals for the addition of cyanogen into the reaction region where H_3^+ has been established by injecting H_2^+ into hydrogen buffer gas upstream. $P = 0.206$ Torr, $\bar{v} = 6.2 \times 10^3$ cm s^{-1}, $L = 45$ cm and $T = 296$ K. H_2^+ is derived from H_2 by electron impact.

into the flow tube giving rise to a variety of secondary and tertiary hydrocarbon ions. The $C_4H_9^+$ and $C_5H_9^+$ ions show only weak decay with the addition of cyanogen into the reaction region and no adducts were observed with these ions. In contrast, $C_3H_5^+$ showed a moderate reaction to produce the adduct $C_3H_5^+ \cdot C_2N_2$ with an apparent bimolecular rate constant of 8×10^{-11} cm^3 molecule^{-1} s^{-1}. The $C_2H_5^+$ ion reacted more rapidly to produce primarily the adduct $C_2H_5^+ \cdot C_2N_2$ with an apparent bimolecular rate constant of 1.6×10^{-10} cm^3 molecule^{-1} s^{-1}. Some $C_2N_2H^+$ appeared to be produced in an uncertain primary reaction. The data allows up to 5% of direct proton transfer with $C_2H_5^+$.

Reactions with protonated cyanogen

The $C_2N_2H^+$ ion could be established in H_2 buffer gas either by injecting $C_2N_2^+$ or by injecting H_2^+ and adding C_2N_2 downstream. There was no evidence for any formation of an adduct with H_2. Table 1 includes a

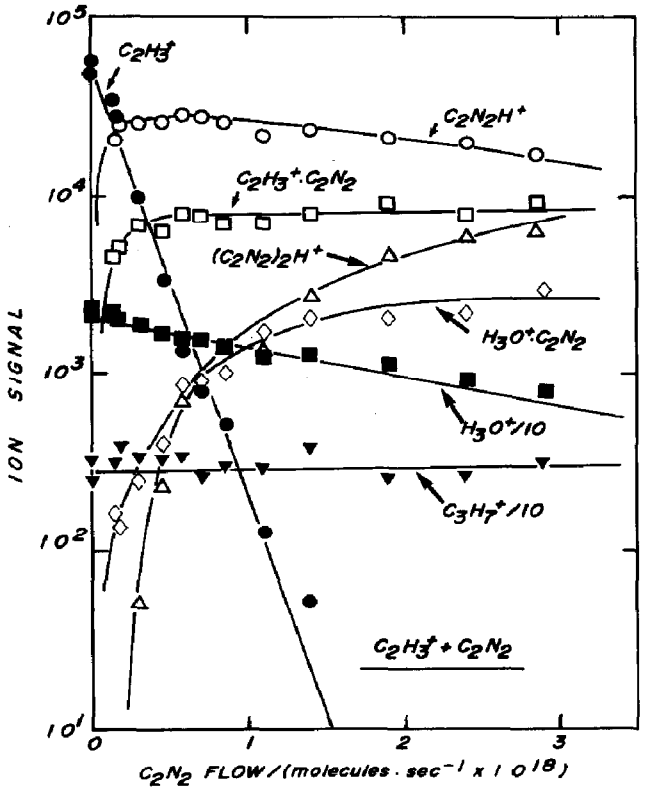

Fig. 3. The observed variation of ion signals for the addition of cyanogen into the reaction region where $C_2H_3^+$ has been established by injection into He buffer gas. $P = 0.317$ Torr, $\bar{v} = 7.1 \times 10^3$ cm s^{-1}, $L = 46$ cm, $T = 295$ K. $C_2H_3^+$ is derived from propylene by electron impact.

summary of the kinetics of the proton-transfer reactions observed with $C_2N_2H^+$.

Rapid proton-transfer reactions were observed with C_2H_4, H_2O and CH_3OH, while adduct formation was observed as the predominant channel with C_2H_2 and SO_2. The study of the reaction with C_2H_2 was complicated by the production of an ion at $m/z = 53$ to levels approaching 10% of the initial signal at $m/z = 53$ due to $C_2N_2H^+$. The $m/z = 53$ ion may arise from the reaction sequence

$$C_2N_2H^+ + C_2H_2 \rightarrow C_4H_3^+ + N_2 \tag{7}$$

$$C_4H_3^+ + H_2 + H_2 \rightarrow C_4H_5^+ + H_2 \tag{8}$$

so that the data allows up to 10% production of $C_4H_3^+$ as a primary reaction channel for the reaction of $C_2N_2H^+$ with C_2H_2. However, a definitive result could not be ascertained because of the presence of impurity ions which could initiate other reaction sequences leading to the same product ion. The

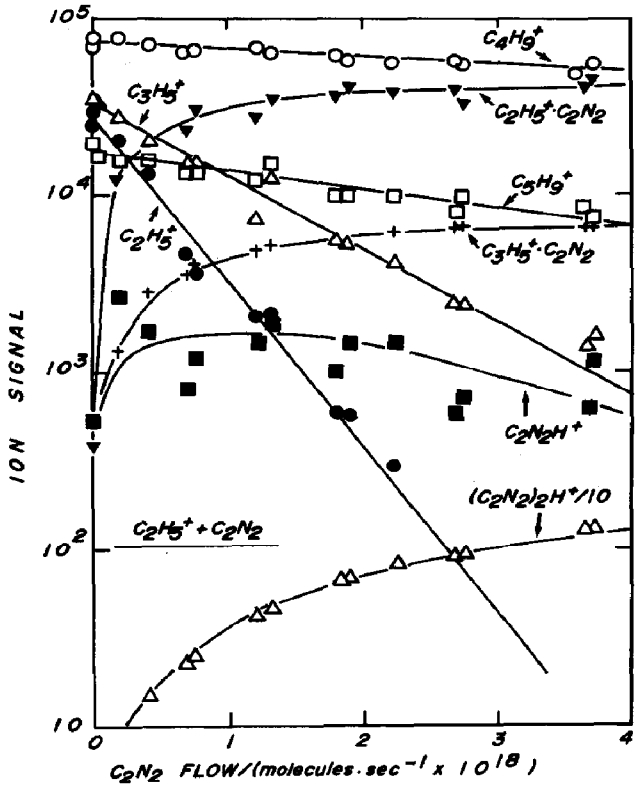

Fig. 4. The observed variation of ion signals for the addition of cyanogen into the reaction region where $C_2H_5^+$ has been established together with other secondary and tertiary ions by injecting H_2^+ into hydrogen buffer gas and adding ethylene upstream. $P = 0.189$ Torr, $\bar{v} = 6.2 \times 10^3$ cm s^{-1}, $L = 45$ cm, $T = 295$ K. H_2^+ is derived from H_2 by electron impact.

results with C_2H_4 are of special interest because, when combined with the results obtained from the reverse reaction of $C_2H_5^+$ with C_2N_2 which indicated a possibility of up to 5% proton transfer, they suggest that the proton affinities of C_2N_2 and C_2H_4 are very nearly equal. The remaining observations also support this conclusion. According to the proton affinities listed in Table 2 the observations indicate that the proton affinity of C_2N_2 lies between those for SO_2 and C_2H_4 and so has a value of 162 ± 2 kcal mol^{-1}. We are not aware of any previous determinations of the proton affinity of cyanogen with which to make a comparison.

Reactions with cyanoacetylene

The proton-transfer reactions observed with cyanoacetylene are indicated in Table 3 along with the measured rate constants. Except for the rate constant obtained with $C_2H_3^+$ there is good agreement with the results reported by Freeman et al. [5] who employed the flowing afterglow method.

TABLE 2

Established proton affinities

Molecule	Proton affinity (kcal mol^{-1})	Ref.
CH_2	197	12 [a]
$(CH_3)_2CO$	194	13
CH_3CN	187 ± 1	13
C_3	184 ± 4	14
CH_3OH	181, 182	12 [a]
CH_3NO_2	181, 180	12 [a]
CH_3CHCH_2	180 ± 2	12 [a]
HCN	171.0 ± 1.7	15
H_2O	165.3 ± 1.8, 166.7	16, 17
C_2H_4	163.0 ± 1.7, 162.6 ± 0.5	16, 17
SO_2	161.2	17
C_2H_2	153.4 ± 2.2	18 [b]
OH	142.3 ± 0.4	12
CO	141.4 ± 0.4	2
N_2	117.4 ± 0.8	2
H_2	100.7 ± 0.8	2

[a] Calculated from thermochemical information therein.
[b] Based on A.P. ($C_2H_3^+$) from C_2H_4.

TABLE 3

Rate constants determined for proton-transfer reactions with $H_2C_3N^+$ or HC_3N using the SIFT technique at 296 ± 2 K

Reaction [a]			Buffer gas	$k_{obs}^{b}/10^{-9}$ (cm^3 molecule^{-1} s^{-1})
$H_3^+ + HC_3N$	$\rightarrow$	$H_2C_3N^+ + H_2$	H_2	10.5 (9.1)
$N_2H^+ + HC_3N$	$\rightarrow$	$H_2C_3N^+ + N_2$	H_2, He	4.2 (4.2)
$HCO^+ + HC_3N$	$\rightarrow$	$H_2C_3N^+ + CO$	He	4.0 (3.7)
$C_2H_3^+ + HC_3N$	$\rightarrow$	$H_2C_3N^+ + C_2H_2$	He	3.9 (1.8)
$H_3O^+ + HC_3N$	$\rightarrow$	$H_2C_3N^+ + H_2O$	H_2, He	3.8 (4.0)
$CH_3NO_2H^+ + HC_3N$	$\xrightarrow{0.5}$	$H_2C_3N^+ + CH_3NO_2$	H_2	1.8
	$\xrightarrow{0.5}$	$(H_4C_4N^+ + HNO_2)$ [c]		
$H_2C_3N^+ + CH_3CN$	$\rightarrow$	$CH_3CNH^+ + HC_3N$	H_2	3.6
$H_2C_3N^+ + (CH_3)_2CO$	$\rightarrow$	$(CH_3)_2COH^+ + HC_3N$	H_2	1.3

[a] The reactions are listed in order of increasing proton removal energy for the reacting ion or proton affinity of the reacting neutral.
[b] The accuracy of the rate constant is estimated to be better than ± 30%. The values in parentheses are those obtained with the flowing afterglow technique as reported in ref. 5.
[c] Other products leading to the formation of an ion with m/z 66 are allowed by stoichiometry.

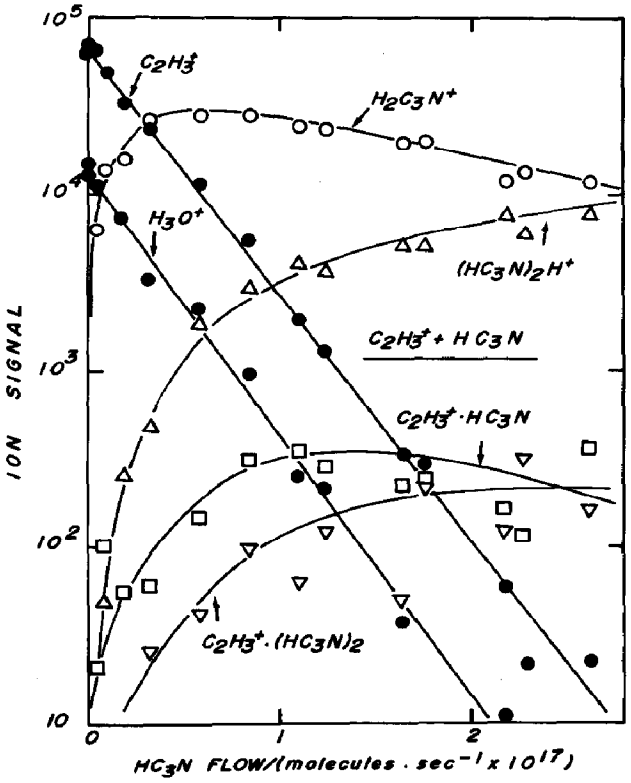

Fig. 5. The observed variation of ion signals for the addition of cyanoacetylene into the reaction region where $C_2H_3^+$ has been established by injection into helium buffer gas. $P = 0.317$ Torr, $\bar{v} = 7.3 \times 10^3$ cm s^{-1}, $L = 46$ cm, $T = 295$ K. $C_2H_3^+$ is derived from propylene by electron impact. The m/z 43 ($C_3H_7^+$) ion is not shown: it is present initially at $\approx 3\%$ of the $C_2H_3^+$ signal and reacts slowly with HC_3N to form the adduct.

The results of one of our experiments with $C_2H_3^+$ are shown in Fig. 5. Clearly, proton transfer is the predominant reaction channel. Some adduct formation to produce $C_2H_3^+ \cdot HC_3N$ was evident but at levels of less than 1% of total product formation. A predominant secondary reaction was the addition reaction to produce $(HC_3N)_2H^+$ and there was some evidence for the addition of a second molecule of cyanoacetylene to $C_2H_3^+$ to form $C_2H_3^+ \cdot (HC_3N)_2$.

The proton-transfer reaction with $CH_3NO_2H^+$ was observed to compete with a channel leading to an ion with m/z 66. Stoichiometry allows a number of different compositions for this ion but, particularly in view of the adduct observed in the reaction of CH_3^+ with cyanoacetylene, we prefer $H_4C_4N^+$ which could arise by elimination of nitrous acid. The NO^+ present in the $CH_3NO_2H^+$ spectrum appeared to react with cyanoacetylene by addition to form $NO^+ \cdot HC_3N$.

The protonated species C_3H^+, CH_3CNH^+ and $(CH_3)_2COH^+$ were all

observed to produce adducts. A $C_3H^+ \cdot HC_3N$ ion was formed in helium at 0.347 Torr (1.1×10^{16} atoms cm^{-3}) with an effective second-order rate constant of 1.3×10^{-9} cm^3 $molecule^{-1}$ s^{-1}. The $CH_3CNH^+ \cdot HC_3N$ and $(CH_3)_2COH^+ \cdot HC_3N$ ions were formed in hydrogen at 0.208 and 0.185 Torr (6.8×10^{15} and 6.0×10^{15} molecules cm^{-3}), respectively, with effective second-order rate constants of 5×10^{-10} and 5×10^{-11} cm^3 $molecule^{-1}$ s^{-1}, respectively. Small fractions ($\sim 3\%$) of an ion at m/z 52 were observed in the primary product spectra of the reactions of C_3H^+ and CH_3CNH^+ but these could be ascribed to reaction involving impurity ions.

The reaction of CH_3^+ with HC_3N is of particular importance. The flowing afterglow measurements reported by Freeman et al. [5] indicated a fast proton-transfer reaction with $k = 2.7 \times 10^{-9}$ cm^3 $molecule^{-1}$ s^{-1}. This observation provided the lower limit to the proton affinity of cyanoacetylene which was reported by these authors to be in the range 197–207 kcal mol^{-1} Figure 6 shows results obtained for this reaction with our SIFT apparatus *.

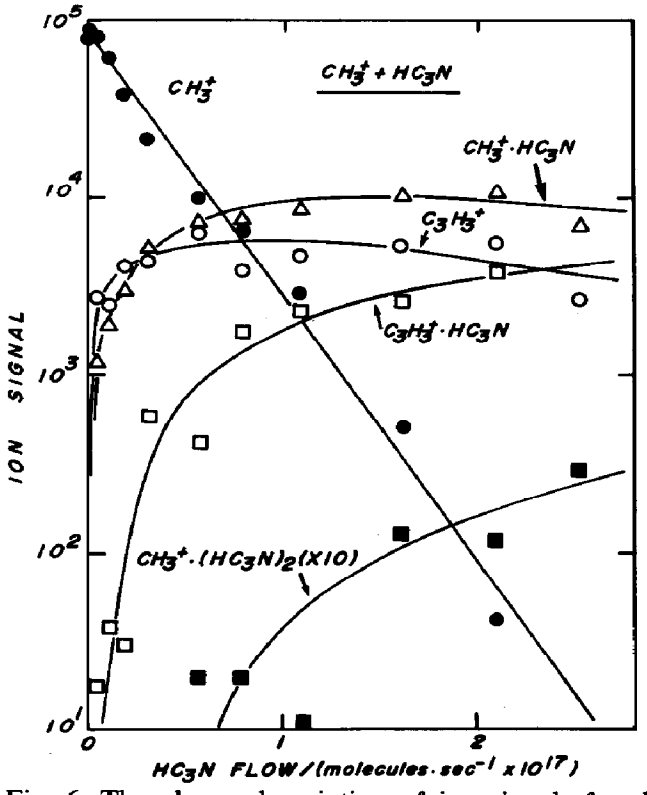

Fig. 6. The observed variation of ion signals for the addition of cyanoacetylene into the reaction region where CH_3^+ has been established by injection into He buffer gas. $P = 0.318$ Torr, $\bar{v} = 7.4 \times 10^3$ cm s^{-1}, $L = 46$ cm, $T = 295$ K. CH_3^+ is derived from CH_4 by electron impact.

* The reaction rate constant was measured to be 4.2×10^{-9} cm^3 $molecule^{-1}$ s^{-1}.

Major products were observed at m/z 39 and 66. Since formation of HC_2N^+ (m/z 39) is endothermic, the reaction channels are

$$CH_3^+ + HC_3N \rightarrow C_3H_3^+ + HCN \quad (9a)$$

$$\rightarrow CH_3^+ \cdot HC_3N \quad (9b)$$

The measured product distribution for (9a) : (9b) was 60 : 40. A m/z 52 ion was observed in the product spectrum at up to 5% of the total product ions but its origin could be attributed entirely to proton-transfer reactions with the impurity ions at m/z 19 (H_3O^+) and m/z 29 (N_2H^+). Failure for the CH_3^+ to react by proton transfer places an *upper* limit to $PA(HC_3N)$ of 197 kcal mol^{-1}. Channel (9a) mimics the observed reaction of CH_3^+ with acetylene to produce $C_3H_3^+$ [10] while channel (9b) corresponds to adduct formation. The two channels appear to reflect the position of attack on the cyanoacetylene molecule: attack at the carbon alpha to the cyanogen group can lead to elimination of HCN and formation of the propargyl cation while attack at the beta carbon would make HCN elimination unfavourable and lead preferentially to the 1, 1-cyanopropenylium adduct ion, CH_3–$CH{=}\overset{+}{C}$–$C{\equiv}N$.

Reactions with protonated cyanoacetylene

The $H_2C_3N^+$ ion was established in H_2 buffer gas either by injecting HC_3N^+ or by injecting H_3^+ and adding HC_3N downstream. An ion with m/z 28 was present in significant amounts when HC_3N^+ was injected. It is likely to have arisen from C_2H^+ produced by the collisional dissociation of HC_3N^+ upon injection. The C_2H^+ ion will quickly convert to $C_2H_4^+$ by successive H-atom transfer and H_2 addition [11]. The presence of the m/z 28 ion can be avoided by injected H_3^+ and adding HC_3N but in this case a clustering reaction also establishes significant amounts of $(HC_3N)_2H^+$.

Table 3 includes the rate constants determined for the fast proton-transfer reactions of $H_2C_3N^+$ with CH_3CN and $(CH_3)_2CO$. Only a very slow addition reaction was observed with C_2H_2 with an effective second-order rate constant $\leqslant 1 \times 10^{-11}$ cm^3 $molecule^{-1}$ s^{-1} at 0.185 Torr in H_2 (6.0×10^{15} molecules s^{-1}). In this case the rate constant measurement was complicated by the presence of an acetone impurity in the acetylene which reacts rapidly with $H_2C_3N^+$. The m/z 28 ($C_2H_4^+$) ion present initially reacted to produce an ion at m/z 39 ($C_3H_3^+$). This is a known reaction with $C_2H_4^+$ [10] and serves to distinguish it from H_2CN^+ (m/z 28). In the experiment with CH_3CN the 'solvated' proton transfer reaction

$$HC_3NH^+ \cdot HC_3N + CH_3CN \rightarrow CH_3CNH^+ \cdot HC_3N + HC_3N \quad (10)$$

was observed to occur with a rate constant of 1.9×10^{-9} cm^3 molecule^{-1} s^{-1}. The results of our experiments with CH_3CN are shown in Fig. 7.

The observed proton-transfer reaction with CH_3CN serves to place an upper limit of 187 ± 1 kcal mol^{-1} on $PA(HC_3N)$. Taken together with the lower limit of 180 kcal mol^{-1} which can be set by the observation of proton transfer between $CH_3NO_2H^+$ and HC_3N, this result leads to a value of 184 ± 4 kcal mol^{-1} for $PA(HC_3N)$.

SUMMARY AND CONCLUSIONS

Three methods were explored for producing protonated species XH^+ with a selected-ion flow tube apparatus fitted with an electron impact ion source: direct production by electron impact at low pressures and indirect production from the reaction of selected X^+ ions with H_2 or the reaction of selected H_2^+ ions with X.

The three methods were applied in measurements of rate constants for

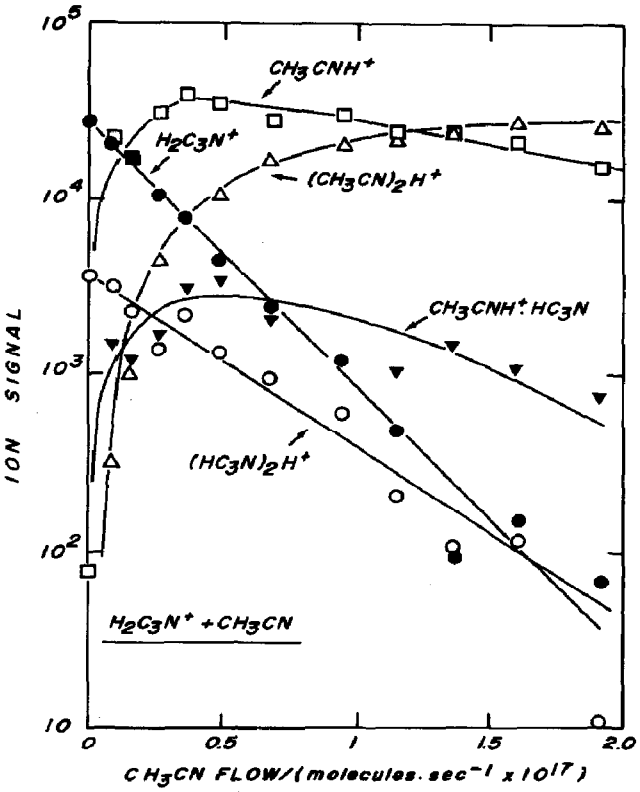

Fig. 7. The observed variation of ion signals for the addition of methyl cyanide into the reaction region where $H_2C_3N^+$ has been established by injecting H_2^+ into H_2 buffer gas and adding cyanoacetylene upstream. $P = 0.204$ Torr, $\bar{v} = 6.3 \times 10^3$ cm s^{-1}, $L = 45$ cm, $T = 295$ K.

proton-transfer reactions of XH^+ with C_2N_2 and HC_3N and of $C_2N_2H^+$ and $H_2C_3N^+$ with X. In a number of cases adduct formation was observed to proceed rapidly.

The observed proton-transfer reactions involving molecules with established proton affinities provide a value for $PA(C_2N_2) = 162 \pm 2$ kcal mol^{-1}. Apparently there has been no previous determination of this quantity.

The observed proton-transfer reactions also provide a value for $PA(HC_3N) = 184 \pm 4$ kcal mol^{-1}. This value is much lower than the value of 202 ± 5 kcal mol^{-1} deduced previously by Freeman et al. [5] using conventional flowing afterglow techniques. The discrepancy arises from the disparity in the flowing afterglow and SIFT observations for the reaction of CH_3^+ with HC_3N. Freeman et al. [5] reported proton transfer as the only channel and used this reaction to provide their lower limit for $PA(HC_3N)$. Our SIFT measurements indicate that formation of $C_3H_3^+ + HCN$ and addition are the dominant reaction channels for this reaction and so it appears to provide an upper limit instead. The lower value for $PA(HC_3N)$ is also more consistent with the results of recent theoretical studies [19]

ACKNOWLEDGEMENTS

We wish to thank Mr. Arnold Fox for helpful discussions and for preparing samples of HC_3N. We thank the Natural Sciences and Engineering Research Council of Canada for financial support.

REFERENCES

1 N.G. Adams and D. Smith, Int. J. Mass Spectrom. Ion Phys., 16 (1975) 167.
2 D.K. Bohme, G.I. Mackay and H.I. Schiff, J. Chem. Phys., 73 (1980) 4976.
3 H.I. Schiff and D.K. Bohme, Astrophys. J., 208 (1976) 237.
4 V.G. Kunde, A.C. Aikin, R.A. Hanel, D.E. Jennings, W.C. Maguire and R.E. Samuelson, Nature (London), 292 (1981) 686.
5 C.G. Freeman, P.W. Harland and M.J. McEwan, Mon. Not. R. Astron. Soc., 187 (1979) 441.
6 G.I. Mackay, G.D. Vlachos, D.K. Bohme and H.I. Schiff, Int. J. Mass Spectrom. Ion Phys., 36 (1980) 259.
7 A.B. Raksit and D.K. Bohme, Int. J. Mass Spectrom. Ion Processes, 55 (1983) 69.
8 G.I. Mackay and D.K. Bohme, Int. J. Mass Spectrom. Ion Phys., 26 (1978) 327.
9 C. Moureu and J.C. Bongrand, Ann. Chim. (Rome), 14 (1920) 47.
10 J.K. Kim, V.G. Anicich and W.T. Huntress, J. Phys. Chem., 81 (1977) 1798.
11 D. Smith and N.G. Adams, Astrophys. J., 217 (1977) 741.
12 H.M. Rosenstock, K. Draxl, B.W. Steiner and J.T. Herron, J. Phys. Chem. Ref. Data, Suppl. 1, 6 (1977).
13 R. Walder and J.L. Franklin, Int. J. Mass Spectrom. Ion Phys., 36 (1980) 85.
14 A.B. Raksit and D.K. Bohme, Int. J. Mass Spectrom. Ion Phys., 49 (1983) 275.
15 K. Tanaka, G.I. Mackay and D.K. Bohme, Can. J. Chem., 56 (1978) 193.
16 D.K. Bohme and G.I. Mackay, J. Am. Chem. Soc., 103 (1981) 2173.
17 S.M. Collyer and T.B. McMahon, J. Phys. Chem., 87 (1983) 909.
18 W.A. Chupka, J. Berkowitz and K.M.A. Refaey, J. Chem. Phys., 50 (1969) 1938.
19 N.N. Haese and R.C. Woods, J. Chem. Phys., 73 (1980) 4521.